ACS SENSORS

Letter

Cite This: ACS Sens. 2018, 3, 72−78

pubs.acs.org/acssensors

Superwettable Electrochemical Biosensor toward Detection of Cancer Biomarkers

Tailin Xu,[†] Yongchao Song,[†] Wei Gao,[#] Tingting Wu,[†] Li-Ping Xu,*[,†] Xueji Zhang,*[,†] and Shutao Wang*[,‡,§]

[†]Research Center for Bioengineering and Sensing Technology, School of Chemistry and Biological Engineering, University of Science and Technology Beijing, Beijing 100083, P. R. China

[‡]CAS Key Laboratory of Bio-inspired Materials and Interfacial Science, CAS Center for Excellence in Nanoscience, Tech-nical Institute of Physics and Chemistry, Chinese Academy of Sciences, Beijing 100190, P. R. China

[§]University of Chinese Academy of Sciences, Beijing 100049, P. R. China

[#]Department of Medical Engineering, California Institute of Technology, Pasadena, California 91125, United States

Supporting Information

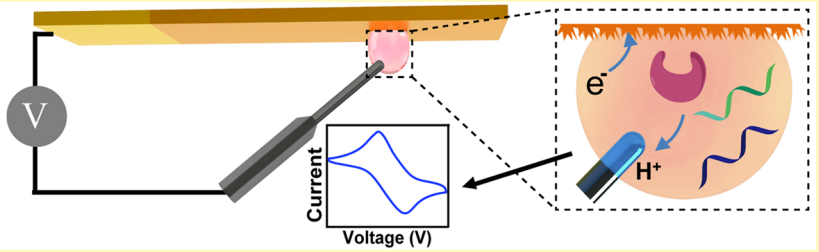

ABSTRACT: Bioinspired superwettable micropatterns that combine two extreme states of superhydrophobicity and superhydrophilicity with the ability to enrich and absorb microdroplets are suitable for versatile and robust sensing applications. Here we introduce a superwettable microchip that integrates superhydrophobic−superhydrophilic micropatterns and a nanodendritic electrochemical biosensor toward the detection of prostate cancer biomarkers. On the superwettable microchip, the superhydrophobic area could confine the microdroplets in superhydrophilic microwells; such behavior is extremely helpful for reducing the amount of analytical solution. In contrast, superhydrophilic microwells exhibit a high adhesive force toward microdroplets, and the nanodendritic structures can improve probe-binding capacity and response signals, thus greatly enhancing the sensitivity. Sensitive and selective detection of prostate cancer biomarkers including miRNA-375, miRNA-141, and prostate-specific antigen on a single microchip is also achieved. Such a superwettable microchip with high sensitivity, low sample volume, and upside-down detection capability in a single microdroplet shows great potential to fabricate portable devices toward complex biosensing applications.

KEYWORDS: *superwettable microchip, superhydrophobic, superhydrophilic, electrochemical sensor, biosensor*

Inspired by extreme states of solid surface wettability in nature, considerable effort has been devoted to the development of materials with superwettable properties for diverse applications.[1−7] Recently, superwettable materials have been proven to have outstanding capacity in controlling liquid droplets, such as their directional motion on anisotropic wettable surface and droplets transferring between surfaces.[8−10] Importantly, superwettable microchips that combine two extreme states of superhydrophobicity and superhydrophilicity in precisely two-dimensional micropatterns[11−14] exhibit excellent ability of patterning microdroplets toward new possibilities and functionalities in a wide variety of biomedical applications including high-throughput cell patterns,[15−18] drug/cell screening,[19−21] and open-channel biochips for separation and diagnostic devices.[22−25] By taking advantage of enrichment and anchoring microdroplet ability of such superwettable microchips, recent efforts have shifted to modify the superhydrophilic microwells with biological entities, toward more versatile and robust sensing applications. As a result, several types of superwettable microchips have been explored depending on different detection signals such as surface-enhanced Raman scattering (SERS),[26−28] colorimetric,[29−33] and fluorescence enhancement effect,[34−36] to perform demanding sensing tasks.[37−39]

Electrochemical biosensors, as one of the most common methods of analytical research, have been widely used to sensitively detect biomolecules,[40−43] such as glucose,[44] nitric oxide,[45] hydrogen peroxide,[46] hydrogen sulfide,[47] DNA/miRNA,[48−50] and proteins.[51] However, electrochemical biosensing is usually carried out in a large solution system. Here

Received: November 22, 2017
Accepted: January 8, 2018
Published: January 8, 2018

DOI: 10.1021/acssensors.7b00868
ACS Sens. 2018, 3, 72−78

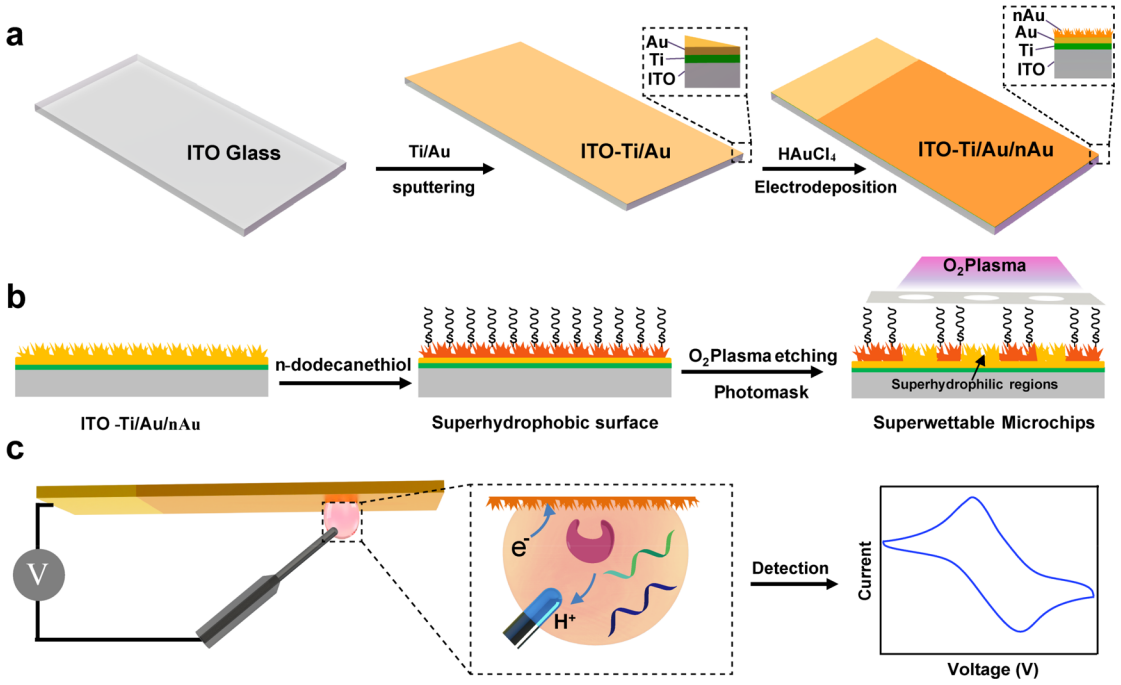

Figure 1. Design of superwettable electrochemical microchip toward biosensing. (a) Fabrication of nanodendritic gold substrate including vapor deposition of Ti/Au thin film and electrochemical deposition gold nanodendrites. (b) Modification of nanodendritic gold substrate to achieve conductive superhydrophobic–superhydrophilic surface. (c) Schematic of electrochemical detection of analyte in droplets on the superwettable electrochemical microchip.

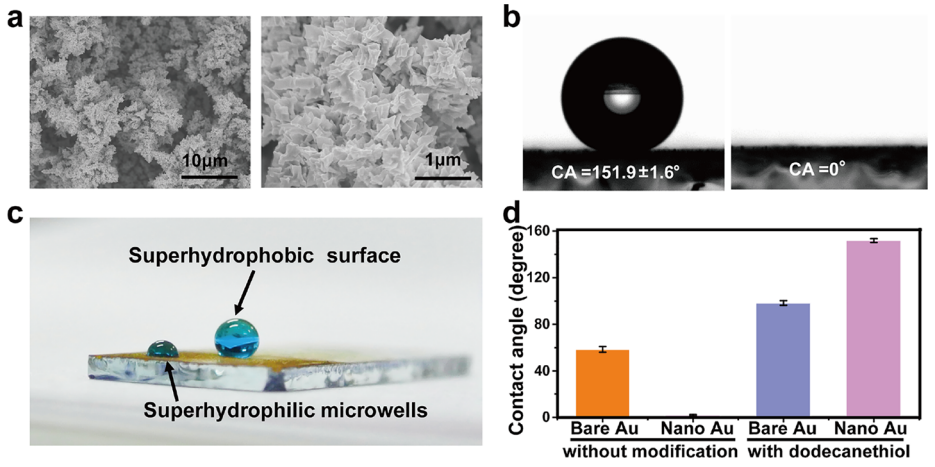

Figure 2. Physical characterization of the superwettable electrochemical microchip. (a) SEM images of the gold nanodendrites. (b) Microscopic images of water contact angle of dodecanethiol modified gold nanodendrites (left) and after O_2 plasma etching (right). (c) Methyl blue labeled water microdroplets behavior on the thiol-modified superhydrophobic gold nanodendrites and on superhydrophilic microwells. (d) Comparison of the contact angles of bare Au and Au nanodendrites before and after the modification of dodecanethoiol.

we demonstrate a superwettable electrochemical biosensor that integrates a superwettable substrate for managing microdroplets with conductive nanodendritic electrochemical biosensor for sensitive measurement, toward detection of multiple prostate cancer biomarkers including miRNA-375, miRNA-141, and prostate-specific antigen. Such a superwettable electrochemical biosensor bridges the gap between sensitive electrochemical biosensing and superwettable droplet management approach, showing great potential in highly sensitive and low-sample-volume detection within a single microdroplet.

By combining electrochemical deposition and template O_2 plasma etching technology, superwettable electrochemical sensors with patterned superhydrophobic–superhydrophilic microarrays were fabricated as detailed in Figure 1. First, the nanodendritic gold substrate was fabricated according to previous literature (see Figure 1a).[52,53] Indium tin oxide (ITO) substrate was cut into small rectangular pieces (1 cm × 2 cm), and ultrasonically cleaned for 10 min in deionized water, acetone, ammonia aqueous, and deionized water sequentially, to remove the organic matters and then dried with a flow of nitrogen. Before electrochemical deposition, a titanium layer and a gold film were sputtered on the conductive side of the ITO substrate to serve as a working electrode for electrochemical deposition processes. Ag/AgCl wire and Pt wire were employed as reference and counter electrodes, respectively. All electrochemical deposition steps were carried out at room

DOI: 10.1021/acssensors.7b00868
ACS Sens. 2018, 3, 72–78

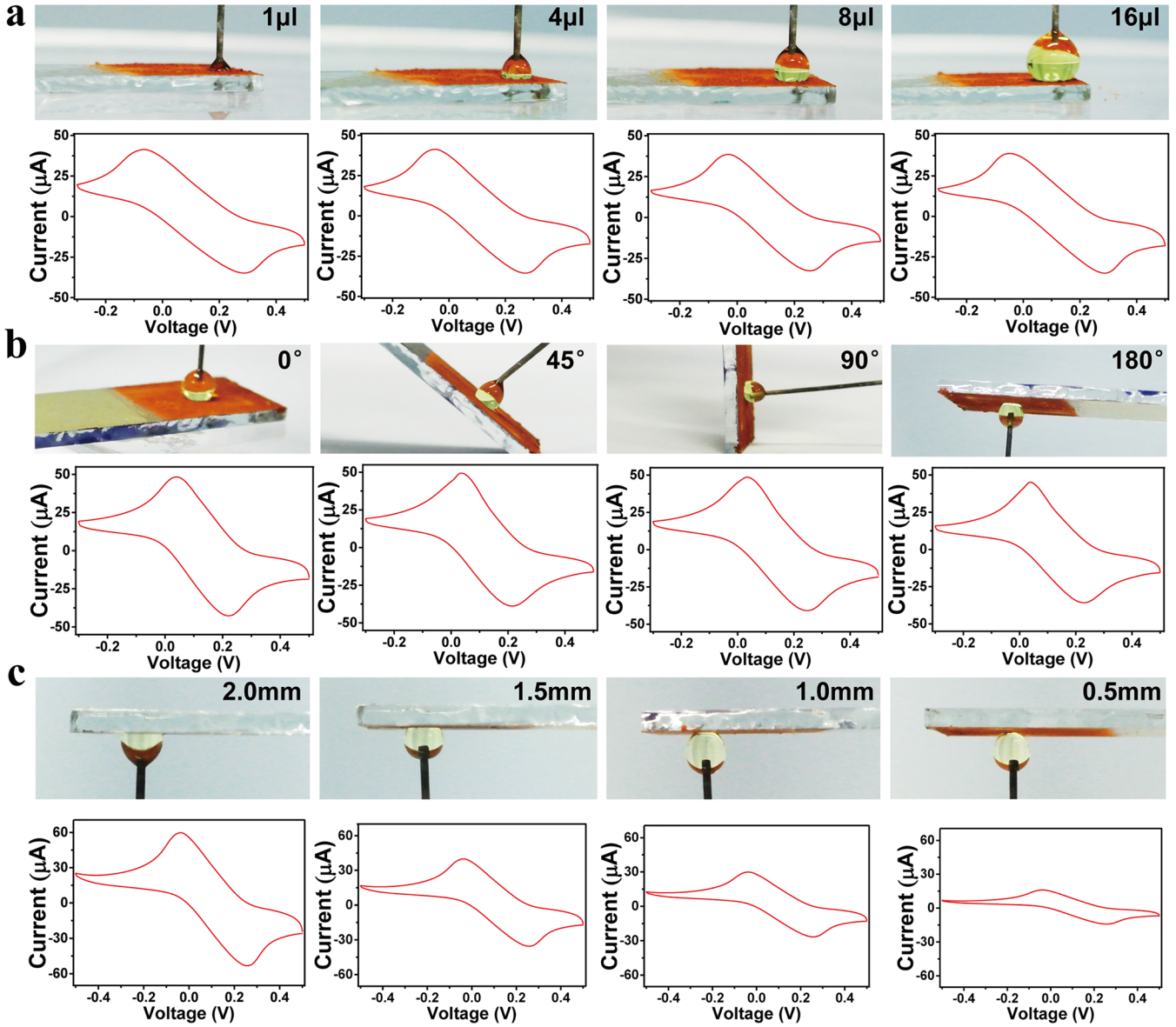

Figure 3. Effect of the microdroplet size, tilting angle, and microwell size on electrochemical redox reactions. (a) Cyclic voltammetry curves (scan rate: 100 mV/s) of superwettable electrode microwells (diameter: 2 mm) with microdroplet volume of 1, 4, 8, and 16 μL, respectively. (b) Rotate the superwettable electrochemical microchip with an angle of 0°, 45°, 90°, and 180° to confirm the stability during the detection processes. (c) Effect of microwell sizes of 0.5, 1.0, 1.5, and 2.0 mm on electrochemical detection. All the measurements were processed in 0.01 M phosphate buffered solution (pH 7.4) containing 0.1 M KCl and 5 mM $K_3[Fe(CN)_6]/K_4[Fe(CN)_6]$.

temperature (25 °C). Gold nanodendritic structures were then electrodeposited at −1.8 V for 1800 s in an electrolyte composed of $HAuCl_4$ (1 mg/mL) and sulfuric acid (0.5 M). After electrochemical deposition, the superhydrophobic−superhydrophilic micropatterns were prepared as shown in Figure 1b. First, the dendritic gold nanostructure was treated with oxygen plasma at 100 W for 180 s for removing the organic matter, and then immersed in a dodecanethiol solution (10 vol % in ethanol) for 24 h at room temperature. The dodecanethiol-modified substrate was cleaned by rinsing in ethanol and ultrapure water, respectively. Oxygen plasma at 100 W was used to irradiate the dodecanethiol-modified substrate through a photomask for 120 s. The nonirradiated region remained superhydrophobic. In contrast, the oxygen plasma irradiated regions became superhydrophilic. Thus, we prepared the superwettable electrochemical biosensor.

The superwettable microchip integrate conductive gold superwettable substrate with electrochemical biosensors, showing great ability of holding microdroplets toward biosensing as shown in Figure 1c. Compared to flat glass without any modifications, the superhydrophilic microwells with nanodendritic structures exhibit a larger adhesive force to hold water microdroplets due to the capillary force of each individual nanostructure. As a result, microdroplets could be captured in the microwell against gravity.[32] In contrast, the dodecanethiol-modified superhydrophobic area prevents water adhering on surface and confines the microdroplets in superhydrophilic microwells, greatly reduceing the amount of analytical solution. In addition, due to the large surface area, multidirectionality, and 3D nanostructure of the nanodendritic electrode surface, the probe-binding capacity and the response signals of the sensor are also greatly improved (SI Figure 2).

DOI: 10.1021/acssensors.7b00868
ACS Sens. 2018, 3, 72−78

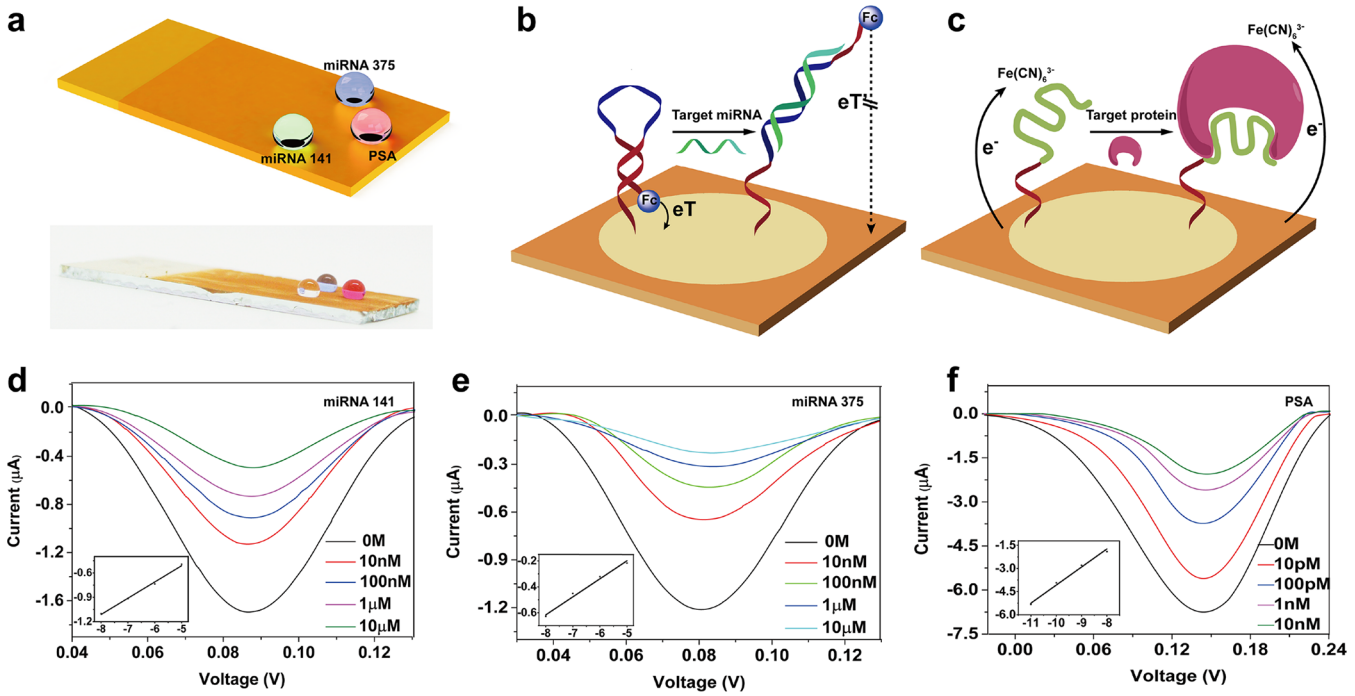

Figure 4. Superwettable microchip toward electrochemical detection of prostate cancer biomarkers. (a) Schematic of superwettable microchip toward detection of prostate cancer biomarkers including miRNA-141, miRNA-375, and prostate-specific antigen. (b) Schematic of electrochemical miRNA sensor comprising an electrode-bound, redox-reporter-modified DNA for target miRNA detection. (c) Schematic of electrochemical aptamer-based sensors (dark blue ribbon) that undergoes a binding-induced conformational change on binding to the target protein (purple sphere). DPV curve for detection of miRNA-141 (d), miRNA-375 (e), and prostate-specific antigen (f).

The gold electrode fabricated by electrochemical deposition method was confirmed by SEM images as illustrated in Figure 2a. The as-prepared electrode exhibited a highly branched structure (about 10−100 nm), the height of these branched structure is up to about 10 μm (SI Figure 1). Figure 2b illustrates the contact angle of gold nanodendrites with or without dodecanethiol modification. Without any modification, the contact angle of gold nanodendrites is about 0° (Figure 2b), while the contact angle of dodecanethiol-modified gold nanodendrites is 151.9 ± 1.6°. Methyl blue labeled microdroplets on the as-prepared substrate present two diametrically opposed appearances as shown in Figure 2c. On the dodecanethiol-modified surface, microdroplet is almost spherical and indicates its superhydrophobicity. In contrast, the microdroplet is flattened in microwells, revealing its superhydrophilicity. In addition, we also evaluated the wettability of bare Au before and after the modification of dodecanethiol (Figure 2d). For Au substrate with or without dodecanethiol modification, the contact angles are 58.6 ± 2.5° and 98.4 ± 2.0°, respectively, which shows a relatively small difference.

To further evaluate the feasibility and versatility of the superwettable electrochemical microchip as a platform toward practical applications, three key parameters closely related to the performance of our superwettable electrochemical microchips including size of the droplet, rotation angle of the microchip, and size of the microwell were chosen to illustrate the ability to perform biodetection.

Figure 3a illustrates the capability of our superwettable electrode microwells toward electrochemical measurement with different microdroplet volumes. Briefly, microdroplets volumes of 1, 4, 8, and 16 μL were then carefully added in the microwells (Diameter: 2 mm). Due to the superhydrophobic propriety of the surrounding area, microdroplets were confined in superhydrophilic microwells and look almost spherical when droplet volume is increased as shown in the optical images. The electrochemical measurement was carried out in 0.01 M phosphate buffered saline (pH = 7.4) containing 0.1 M KCl and 5 mM potassium ferricyanide/ferrocyanide. Cyclic voltammetry results (scan rate: 100 mV/s) of microdroplets with of 1, 4, 8, and 16 μL are just subtly different, revealing the stability of such a superwettable microchip toward biodetection regardless of the droplet size. Figure 3b demonstrates the adhesive property to microdroplet of such superwettable microchip to confirm its capability toward upside-down measurement during the detection process. In brief, the superwettable electrochemical microchip with a microwell of 2 mm was first horizontally placed, 5 μL microdroplet which contained 0.01 M phosphate buffered saline and 0.1 M potassium ferricyanide/ferrocyanide were then carefully added in the microwells (0°). When the superwettable electrochemical microchip are rotated with angles of 45°, 90°, and 180°, the water droplets can be anchored at the microwells without dropping down due to the large capillary force of such a superhydrophilic microwell as demonstrated in optical images. Cyclic voltammetry curves are almost the same with different tilting angles, revealing the stability of such superwettable microchip. Such a non-angle-dependent electrochemical device shows great potential in fabricating portable device. In Figure 3c, the influence of the microwell size on the electrochemical response of superwettable microchip was demonstrated. The electrochemical measurement was carried out in the reversed microchip, which is much more conducive to observation. 5 μL microdroplet (0.01 M phosphate buffered saline and 0.1 M potassium ferricyanide-/ferrocyanide) were carefully added in the reversed microwells. With the microwell sizes decreasing from 2.0 mm to 0.5 mm, the microwells keep

DOI: 10.1021/acssensors.7b00868
ACS Sens. 2018, 3, 72−78

anchoring microdroplets as shown in the optical images. However, the contact area between the microdroplet and the microwell has a significant influence on probe-binding capacity and the response signals, in which the signal decreases as the contact area decreases.

For electrochemical detection of miRNA and protein, a two-electrode system where Ag/AgCl acts as both reference and counter electrode is chosen to simplify design and suit the small size of the microdroplets, which is a common strategy for low-current and low-volume electrochemical sensing.[54] Two kinds of typical prostate cancer biomarkers including miRNAs (miRNA-141 and miRNA-375[55,56]) and prostate-specific antigen (PSA)[57] were chosen to illustrate the ability to perform biodetection to further evaluate its feasibility and versatility as a platform toward sensitive biosensing as demonstrated in Figure 4a. Such multivariate analyses of the PSA and miRNA levels are able to enhance the performance in detecting prostate cancer.

The mechanism of the superwettable microchip for electrochemical miRNA sensing is illustrated in Figure 4b. The miRNA sensors comprise an electrode-bound, redox-reporter-modified DNA probe (purple-blue-purple ribbon) that undergoes a conformational change on binding to the target miRNA (bluish green ribbon). This conformational change alters the positioning of the reporter (Fc) relative to the electrode surface, thereby producing a target-dependent change in current when the sensor is interrogated by differential pulse voltammetry (DPV). The detailed detection processes were carried out at constant temperature and saturated humidity as follows: a 5 μL water droplet with 10.0 μM DNA probe was dropped in a superhydrophilic microwell (diameter: 2 mm), and incubated at room temperature for probe DNA self-assembly and automatically ringing on the nanodendritic gold surface. Prior to measurement, the microchip was immersed in ultrapure water to remove unfixed DNA. Then, a 5 μL water microdroplet (pH 7.0) contains 140 mM NaCl, 100 mM $NaClO_4$, and target miRNA concentrations of 0 M, 10 nM, 100 nM, 1 μM, and 10 μM were dropped in microwells for 30 min to ensure the sufficient hybridization of DNA probe and target miRNA. The detection of miRNA-141 and miRNA-375 was performed by DPV (voltage varies from −0.0 V to +0.14 V) as demonstrated in Figure 4d and e, respectively. The response signals decrease as the concentration of target miRNA increases. A linear plot of the signal peak point (0.08 V) versus the target miRNA-141 and miRNA-375 concentration ranging from 10 nm to 10 μM was established and a detection limit at a signal-to-noise ratio of 3 was calculated to be 0.8 nM.

The detection of PSA was carried out by immobilizing aptamer onto the superhydrophilic microwell as shown in Figure 4c. The PSA sensors comprise an electrode-bound aptamer (purple-blue ribbon) for binding the target protein (purple sphere). Such protein−aptamer binding alters the positioning of the reporter (potassium ferricyanide) relative to the electrode surface, thereby producing a target-dependent change in current. The detailed detection procedure for target protein detection was carried out almost the same as miRNA: a 5 μL water microdroplet (pH 7.0) containing 1 mM $C_{11}H_{12}FeO$, 1 mM $MgCl_2$, and 140 mM NaCl, and target PSA concentrations of 0 M, 10 pM, 100 pM, 1 nM, and 10 nM were dropped in microwells. Due to the aptamer's specific recognition, the corresponding response signals were gradually decreasing upon the increasing target PSA concentration as demonstrated in Figure 4f. A linear plot of the signal peak point (0.014 V) versus concentration of target protein is ranging from 10 pm to 10 nM with a detection limit of 1.0 pM.

To evaluate the practical application and the selectivity of the biosensor, the goat serum (containing various proteins, 1:10 diluted with 0.1 M PBS) was used as electrolyte to detect the PSA and miRNA (detailed in Supporting Information).[58,59] The selectivity of the superwettable microchip in serum sample as shown in SI Figure 3. When immobilized with detection probe for miRNA-141, the superwettable microchip can just respond to target miRNA-141 regardless of adding miRNA-375 and PSA (SI Figure 3a). Meanwhile, the superwettable microchip can only respond to target PSA when functionalized with PSA aptamer (SI Figure 3b). Such results revealed the potential of this superwettable biosensor toward practical application.

In conclusion, the superwettable microchip sensor described in this study represents a hybrid system that integrates a superwettable substrate for microdroplet management with nanodendritic gold electrochemical biosensor for sensitive measurement into a single microdroplet detection platform, which overcomes limitations of conventional electrochemical sensors. Such a microchip is realized via electrochemical deposition for nanodendritic gold structure, dodecanethiol modification for superhydrophobic surface, and template O_2 plasma etching for superhydrophilic microwells. A microliter of analytical solution can be utilized during detection processes due to the superhydrophobicity of the surface. The conductive nanodendritic structures in superhydrophilic microwells can effectively enhance the sensitivity and exhibit a high adhesive property. Such capability allows the superwettable microchip to be a biosensing platform in sensitive detection of routine prostate cancer biomarkers including miRNA-375, miRNA-141, and prostate-specific antigen. Such a superwettable microchip represents a great opportunity to manipulate microdroplets toward a precise decease in detection based on multivariate analysis on a single microchip.

■ ASSOCIATED CONTENT

Supporting Information

The Supporting Information is available free of charge on the ACS Publications website at DOI: 10.1021/acssensors.7b00868.

Experimental details, oligonucleotides sequences, electrochemical performance comparison of nanodendritic Au and bare Au electrode, additional figures (PDF)

■ AUTHOR INFORMATION

Corresponding Authors

*E-mail: xuliping@ustb.edu.cn.
*E-mail: zhangxueji@ustb.edu.cn.
*E-mail: stwang@mail.ipc.ac.cn.

ORCID

Tailin Xu: 0000-0003-4037-2856
Shutao Wang: 0000-0002-2559-5181

Author Contributions

X.T. and S.Y. contributed equally to this work.

Notes

The authors declare no competing financial interest.

DOI: 10.1021/acssensors.7b00868
ACS Sens. 2018, 3, 72−78

■ ACKNOWLEDGMENTS

The work is supported by National Natural Science Foundation of China (NSFC Grant no. 21475009, 21727815), the Top-Notch Young Talents Program of China, and Beijing Municipal Science & Technology Commission (Z131102002813058, Z161100000116037), Fundamental Research Funds for the Central Universities (FRF-TP-17-066A1), Natural Science Foundation of Beijing (2184109).

■ REFERENCES

(1) Wang, S. T.; Liu, K. S.; Yao, X.; Jiang, L. Bioinspired Surfaces with Superwettability: New Insight on Theory, Design, and Applications. *Chem. Rev.* **2015**, *115*, 8230−8293.
(2) Celia, E.; Darmanin, T.; Taffin de Givenchy, E.; Amigoni, S.; Guittard, F. Recent advances in designing superhydrophobic surfaces. *J. Colloid Interface Sci.* **2013**, *402*, 1−18.
(3) Gauthier, A.; Symon, S.; Clanet, C.; Quere, D. Water impacting on superhydrophobic macrotextures. *Nat. Commun.* **2015**, *6*, 8001.
(4) Kreder, M. J.; Alvarenga, J.; Kim, P.; Aizenberg, J. Design of anti-icing surfaces: smooth, textured or slippery? *Nat. Rev. Mater.* **2016**, *1*, 15003.
(5) Liu, M.; Wang, S.; Jiang, L. Nature-inspired superwettability systems. *Nat. Rev. Mater.* **2017**, *2*, 17036.
(6) Deng, X.; Mammen, L.; Butt, H. J.; Vollmer, D. Candle soot as a template for a transparent robust superamphiphobic coating. *Science* **2012**, *335*, 67−70.
(7) Li, X. M.; Reinhoudt, D.; Crego-Calama, M. What do we need for a superhydrophobic surface? A review on the recent progress in the preparation of superhydrophobic surfaces. *Chem. Soc. Rev.* **2007**, *36*, 1350−1368.
(8) Zheng, Y.; Bai, H.; Huang, Z.; Tian, X.; Nie, F. Q.; Zhao, Y.; Zhai, J.; Jiang, L. Directional water collection on wetted spider silk. *Nature* **2010**, *463*, 640−643.
(9) Lv, J. A.; Liu, Y.; Wei, J.; Chen, E.; Qin, L.; Yu, Y. Photocontrol of fluid slugs in liquid crystal polymer microactuators. *Nature* **2016**, *537*, 179−184.
(10) Tian, X.; Verho, T.; Ras, R. H. Moving superhydrophobic surfaces toward real-world applications. *Science* **2016**, *352*, 142−143.
(11) Zhang, X.; Jin, M.; Liu, Z.; Tryk, D. A.; Nishimoto, S.; Murakami, T.; Fujishima, A. Superhydrophobic TiO2 Surfaces: Preparation, Photocatalytic Wettability Conversion, and Superhydrophobic−Superhydrophilic Patterning. *J. Phys. Chem. C* **2007**, *111*, 14521−14529.
(12) Zahner, D.; Abagat, J.; Svec, F.; Frechet, J. M.; Levkin, P. A. A facile approach to superhydrophilic-superhydrophobic patterns in porous polymer films. *Adv. Mater.* **2011**, *23*, 3030−3034.
(13) Tian, D.; Song, Y.; Jiang, L. Patterning of controllable surface wettability for printing techniques. *Chem. Soc. Rev.* **2013**, *42*, 5184−5209.
(14) Gu, Z.-Z.; Fujishima, A.; Sato, O. Patterning of a Colloidal Crystal Film on a Modified Hydrophilic and Hydrophobic Surface. *Angew. Chem.* **2002**, *114*, 2171.
(15) Ito, Y. Surface micropatterning to regulate cell functions. *Biomaterials* **1999**, *20*, 2333−2342.
(16) Shi, W.; Xu, T.; Xu, L. P.; Chen, Y.; Wen, Y.; Zhang, X.; Wang, S. Cell micropatterns based on silicone-oil-modified slippery surfaces. *Nanoscale* **2016**, *8*, 18612−18615.
(17) Geyer, F. L.; Ueda, E.; Liebel, U.; Grau, N.; Levkin, P. A. Superhydrophobic-superhydrophilic micropatterning: towards genome-on-a-chip cell microarrays. *Angew. Chem., Int. Ed.* **2011**, *50*, 8424−8427.
(18) Efremov, A. N.; Stanganello, E.; Welle, A.; Scholpp, S.; Levkin, P. A. Micropatterned superhydrophobic structures for the simultaneous culture of multiple cell types and the study of cell-cell communication. *Biomaterials* **2013**, *34*, 1757−1763.
(19) Oliveira, M. B.; Neto, A. I.; Correia, C. R.; Rial-Hermida, M. I.; Alvarez-Lorenzo, C.; Mano, J. F. Superhydrophobic Chips for Cell Spheroids High-Throughput Generation and Drug Screening. *ACS Appl. Mater. Interfaces* **2014**, *6*, 9488−9495.
(20) Popova, A. A.; Schillo, S. M.; Demir, K.; Ueda, E.; Nesterov-Mueller, A.; Levkin, P. A. Droplet-Array (DA) Sandwich Chip: A Versatile Platform for High-Throughput Cell Screening Based on Superhydrophobic-Superhydrophilic Micropatterning. *Adv. Mater.* **2015**, *27*, 5217−5222.
(21) Leite, Á. J.; Oliveira, M. B.; Caridade, S. G.; Mano, J. F. Screening of Nanocomposite Scaffolds Arrays Using Superhydrophobic-Wettable Micropatterns. *Adv. Funct. Mater.* **2017**, *27*, 1701219.
(22) Parolo, C.; Merkoci, A. Paper-based nanobiosensors for diagnostics. *Chem. Soc. Rev.* **2013**, *42*, 450−457.
(23) Shang, L.; Cheng, Y.; Zhao, Y. Emerging Droplet Microfluidics. *Chem. Rev.* **2017**, *117*, 7964−8040.
(24) Neto, A. I.; Demir, K.; Popova, A. A.; Oliveira, M. B.; Mano, J. F.; Levkin, P. A. Fabrication of Hydrogel Particles of Defined Shapes Using Superhydrophobic-Hydrophilic Micropatterns. *Adv. Mater.* **2016**, *28*, 7613−7619.
(25) Garcia-Cordero, J. L.; Fan, Z. H. Sessile droplets for chemical and biological assays. *Lab Chip* **2017**, *17*, 2150−2166.
(26) De Angelis, F.; Gentile, F.; Mecarini, F.; Das, G.; Moretti, M.; Candeloro, P.; Coluccio, M. L.; Cojoc, G.; Accardo, A.; Liberale, C.; Zaccaria, R. P.; Perozziello, G.; Tirinato, L.; Toma, A.; Cuda, G.; Cingolani, R.; Di Fabrizio, E. Breaking the diffusion limit with super-hydrophobic delivery of molecules to plasmonic nanofocusing SERS structures. *Nat. Photonics* **2011**, *5*, 682−687.
(27) Lu, L.-Q.; Zheng, Y.; Qu, W.-G.; Yu, H.-Q.; Xu, A.-W. Hydrophobic Teflon films as concentrators for single-molecule SERS detection. *J. Mater. Chem.* **2012**, *22*, 20986.
(28) Shin, S.; Lee, J.; Lee, S.; Kim, H.; Seo, J.; Kim, D.; Hong, J.; Lee, S.; Lee, T. A Droplet-Based High-Throughput SERS Platform on a Droplet-Guiding-Track-Engraved Superhydrophobic Substrate. *Small* **2017**, *13*, 1 DOI: 10.1002/smll.201770037.
(29) Hou, J.; Zhang, H.; Yang, Q.; Li, M.; Jiang, L.; Song, Y. Hydrophilic-Hydrophobic Patterned Molecularly Imprinted Photonic Crystal Sensors for High-Sensitive Colorimetric Detection of Tetracycline. *Small* **2015**, *11*, 2738−2742.
(30) Wu, T.; Xu, T.; Xu, L. P.; Huang, Y.; Shi, W.; Wen, Y.; Zhang, X. Superhydrophilic cotton thread with temperature-dependent pattern for sensitive nucleic acid detection. *Biosens. Bioelectron.* **2016**, *86*, 951−957.
(31) Zhang, Y.; Ren, T.; Li, T.; He, J.; Fang, D. Paper-Based Hydrophobic/Lipophobic Surface for Sensing Applications Involving Aggressive Liquids. *Adv. Mater. Interfaces* **2016**, *3*, 1600672.
(32) Xu, T.; Shi, W.; Huang, J.; Song, Y.; Zhang, F.; Xu, L. P.; Zhang, X.; Wang, S. Superwettable Microchips as a Platform toward Microgravity Biosensing. *ACS Nano* **2017**, *11*, 621−626.
(33) Hernandez-Perez, R.; Fan, Z. H.; Garcia-Cordero, J. L. Evaporation-Driven Bioassays in Suspended Droplets. *Anal. Chem.* **2016**, *88*, 7312−7317.
(34) Hou, J.; Zhang, H.; Yang, Q.; Li, M.; Song, Y.; Jiang, L. Bioinspired photonic-crystal microchip for fluorescent ultratrace detection. *Angew. Chem., Int. Ed.* **2014**, *53*, 5791−5795.
(35) Yen, T. M.; Zhang, T.; Chen, P. W.; Ku, T. H.; Chiu, Y. J.; Lian, I.; Lo, Y. H. Self-Assembled Pico-Liter Droplet Microarray for Ultrasensitive Nucleic Acid Quantification. *ACS Nano* **2015**, *9*, 10655−10663.
(36) Xu, L. P.; Chen, Y.; Yang, G.; Shi, W.; Dai, B.; Li, G.; Cao, Y.; Wen, Y.; Zhang, X.; Wang, S. Ultratrace DNA Detection Based on the Condensing-Enrichment Effect of Superwettable Microchips. *Adv. Mater.* **2015**, *27*, 6878−6884.
(37) Falde, E. J.; Yohe, S. T.; Colson, Y. L.; Grinstaff, M. W. Superhydrophobic materials for biomedical applications. *Biomaterials* **2016**, *104*, 87−103.
(38) Shin, S.; Seo, J.; Han, H.; Kang, S. B.; Kim, H.; Lee, T. Bio-Inspired Extreme Wetting Surfaces for Biomedical Applications. *Materials* **2016**, *9*, 116.

DOI: 10.1021/acssensors.7b00868
ACS Sens. 2018, 3, 72−78

(39) Ueda, E.; Levkin, P. A. Emerging applications of superhydrophilic-superhydrophobic micropatterns. *Adv. Mater.* **2013**, *25*, 1234−1247.
(40) Wang, P.; Lin, Z.; Su, X.; Tang, Z. Application of Au based nanomaterials in analytical science. *Nano Today* **2017**, *12*, 64−97.
(41) Zheng, G.; Patolsky, F.; Cui, Y.; Wang, W. U.; Lieber, C. M. Multiplexed electrical detection of cancer markers with nanowire sensor arrays. *Nat. Biotechnol.* **2005**, *23*, 1294−1301.
(42) Chen, A.; Chatterjee, S. Nanomaterials based electrochemical sensors for biomedical applications. *Chem. Soc. Rev.* **2013**, *42*, 5425−5438.
(43) Song, S.; Qin, Y.; He, Y.; Huang, Q.; Fan, C.; Chen, H. Y. Functional nanoprobes for ultrasensitive detection of biomolecules. *Chem. Soc. Rev.* **2010**, *39*, 4234−4243.
(44) Wang, J. Electrochemical glucose biosensors. *Chem. Rev.* **2008**, *108*, 814−825.
(45) Xu, T.; Scafa, N.; Xu, L.-P.; Su, L.; Li, C.; Zhou, S.; Liu, Y.; Zhang, X. Electrochemical Sensors for Nitric Oxide Detection in Biological Applications. *Electroanalysis* **2014**, *26*, 449−468.
(46) Chen, W.; Cai, S.; Ren, Q. Q.; Wen, W.; Zhao, Y. D. Recent advances in electrochemical sensing for hydrogen peroxide: a review. *Analyst* **2012**, *137*, 49−58.
(47) Xu, T.; Scafa, N.; Xu, L. P.; Zhou, S.; Abdullah Al-Ghanem, K.; Mahboob, S.; Fugetsu, B.; Zhang, X. Electrochemical hydrogen sulfide biosensors. *Analyst* **2016**, *141*, 1185−1195.
(48) Fan, C.; Plaxco, K. W.; Heeger, A. J. Electrochemical interrogation of conformational changes as a reagentless method for the sequence-specific detection of DNA. *Proc. Natl. Acad. Sci. U. S. A.* **2003**, *100*, 9134−9137.
(49) Das, J.; Ivanov, I.; Montermini, L.; Rak, J.; Sargent, E. H.; Kelley, S. O. An electrochemical clamp assay for direct, rapid analysis of circulating nucleic acids in serum. *Nat. Chem.* **2015**, *7*, 569−575.
(50) Drummond, T. G.; Hill, M. G.; Barton, J. K. Electrochemical DNA sensors. *Nat. Biotechnol.* **2003**, *21*, 1192−1199.
(51) Wen, W.; Yan, X.; Zhu, C.; Du, D.; Lin, Y. Recent Advances in Electrochemical Immunosensors. *Anal. Chem.* **2017**, *89*, 138−156.
(52) Zhang, X.; Shi, F.; Yu, X.; Liu, H.; Fu, Y.; Wang, Z.; Jiang, L.; Li, X. Polyelectrolyte multilayer as matrix for electrochemical deposition of gold clusters: toward super-hydrophobic surface. *J. Am. Chem. Soc.* **2004**, *126*, 3064−3065.
(53) Soleymani, L.; Fang, Z.; Sargent, E. H.; Kelley, S. O. Programming the detection limits of biosensors through controlled nanostructuring. *Nat. Nanotechnol.* **2009**, *4*, 844−848.
(54) Gao, W.; Emaminejad, S.; Nyein, H. Y. Y.; Challa, S.; Chen, K.; Peck, A.; Fahad, H. M.; Ota, H.; Shiraki, H.; Kiriya, D.; Lien, D.-H.; Brooks, G. A.; Davis, R. W.; Javey, A. Fully integrated wearable sensor arrays for multiplexed in situ perspiration analysis. *Nature* **2016**, *529*, 509−514.
(55) Sita-Lumsden, A.; Dart, D. A.; Waxman, J.; Bevan, C. L. Circulating microRNAs as potential new biomarkers for prostate cancer. *Br. J. Cancer* **2013**, *108*, 1925−1930.
(56) Bryant, R. J.; Pawlowski, T.; Catto, J. W.; Marsden, G.; Vessella, R. L.; Rhees, B.; Kuslich, C.; Visakorpi, T.; Hamdy, F. C. Changes in circulating microRNA levels associated with prostate cancer. *Br. J. Cancer* **2012**, *106*, 768−774.
(57) Perfezou, M.; Turner, A.; Merkoci, A. Cancer detection using nanoparticle-based sensors. *Chem. Soc. Rev.* **2012**, *41*, 2606−2622.
(58) Liu, J.; Wang, X.; Wang, T.; Li, D.; Xi, F.; Wang, J.; Wang, E. Functionalization of monolithic and porous three-dimensional graphene by one-step chitosan electrodeposition for enzymatic biosensor. *ACS Appl. Mater. Interfaces* **2014**, *6*, 19997−20002.
(59) Niu, X.; Chen, C.; Zhao, H.; Chai, Y.; Lan, M. Novel snowflake-like Pt-Pd bimetallic clusters on screen-printed gold nanofilm electrode for H2O2 and glucose sensing. *Biosens. Bioelectron.* **2012**, *36*, 262−266.

DOI: 10.1021/acssensors.7b00868
ACS Sens. 2018, 3, 72−78